SORT 44 (1) January-June 2020, 141-170 DOI: 10.2436/20.8080.02.98

Green hybrid fleets using electric vehicles: solving the heterogeneous vehicle routing problem with multiple driving ranges and loading capacities

Sara Hatami[1], Majid Eskandarpour[2], Manuel Chica[3,4], Angel A. Juan[1] and Djamila Ouelhadj[5]

Abstract

The introduction of Electric Vehicles (EVs) in modern fleets facilitates green road transportation. However, the driving ranges of EVs are limited by the duration of their batteries, which arise new operational challenges. Hybrid fleets of gas and EVs might be heterogeneous both in loading capacities as well as in driving-range capabilities, which makes the design of efficient routing plans a difficult task. In this paper, we propose a new Multi-Round Iterated Greedy (MRIG) metaheuristic to solve the Heterogeneous Vehicle Routing Problem with Multiple Driving ranges and loading capacities (HeVRPMD). MRIG uses a successive approximations method to offer the decision maker a set of alternative fleet configurations, with different distance-based costs and green levels. The numerical experiments show that MRIG is able to outperform previous works dealing with the homogeneous version of the problem, which assumes the same loading capacity for all vehicles in the fleet. The numerical experiments also confirm that the proposed MRIG approach extends previous works by solving a more realistic HeVRPMD and provides the decision-maker with fleets with higher green levels.

MSC: 90B06, 90C59, 68W20, 62P12.

Keywords: Vehicle Routing Problem, Electric Vehicles, Heterogeneous Fleet, Multiple Driving Ranges. Iterated Greedy heuristic, Successive Approximations Method

1 Introduction

Transportation is one of the main activities in modern supply chains, and accordingly, it has a significant effect on the customer level of satisfaction (Crainic, 2000). Likewise, CO_2 and greenhouse-gas emissions play an important role in producing the side

[1] IN3 – Computer Science Dept., Universitat Oberta de Catalunya, Barcelona, Spain, ajuanp@uoc.edu

[2] IÉSEG School of Management, Université de Lille, France

[3] Andalusian Research Institute DaSCI, University of Granada, Granada, Spain

[4] School of Electrical Engineering and Computing, University of Newcastle, Australia

[5] Centre for OR and Logistics, School of Math and Physics, University of Portsmouth, Portsmouth, UK

Received: June 2019
Accepted: May 2020

effects (externalities) of noise pollution, air pollution, and traffic congestion (Faulin et al., 2019). Therefore, enterprises must consider both customer satisfaction and environmental impact when planning their transportation operations. In fact, some governments are making noticeable efforts for promoting 'green' (environment-friendly) policies. One of these policies is related to shifting from Internal-Combustion-Engine Vehicles (ICEVs) to zero-emission Electric Vehicles (EVs) or, at least, to Plug-in Hybrid Electric Vehicles (PHEVs) (Mattila and Antikainen, 2011). Both ICEVs and PHEVs consume oil and produce a higher percentage of CO_2, greenhouse emissions, and other pollutant effects compared to EVs. It is then clear that a shift from a fossil fuel fleet to an electric-powered fleet is necessary to reduce pollutant emissions in cities. Also, by introducing special taxes, governments are approving policies aimed at decreasing the pollution level generated by transportation (Faulin, Lera-López and Juan, 2011). Other ways of promoting green technologies refer to offer incentives for companies to reduce carbon footprint, diminish the risk associated with the dependence on oil-based energy sources, make more affordable the acquisition of EVs, and develop alternative-energy technologies (Williams et al., 2012). Therefore, from both an environmental and energy standpoints, the use of EVs should be a first priority for the reduction of primary energy consumption.

Although EVs show many advantages regarding the use of a greener energy, this technology is currently facing some drawbacks. In particular, these vehicles make use of electronic batteries, which limit their driving-range capabilities. These batteries have long-recharge processing times and cannot be charged in classical service stations on the road (Chan et al., 2009; Wirasingha, Schofield and Emadi, 2008; Ferreira et al., 2011; Achtnicht, Bühler and Hermeling, 2012). On the contrary, the driving ranges of ICEVs and PHEVs are assumed to be unlimited as they can be easily refueled at any station along their route. With EVs becoming more prevalent among current fleets of vehicles, an efficient routing of hybrid fleets of vehicles with multiple driving-ranges is an emergent challenge in the transportation industry. Thus, the Vehicle Routing Problem with Multiple Driving ranges (VRPMD) takes into account a hybrid fleet of EVs, PHEVs, and ICEVs. However, the different vehicles of the fleet are assumed to have the same loading capacity.

In this paper, we propose a more realistic model by also considering heterogeneous fleets of vehicles in terms of loading capacity and driving ranges. The novel model is called the Heterogeneous Vehicle Routing Problem with Multiple Driving ranges (HeVRPMD). To solve this new model, we propose a Multi-Round Iterated Greedy (MRIG) metaheuristic based on a successive approximations method. The final solution for the heterogeneous case is obtained by solving a series of homogeneous cases and then combining the resulting partial solutions into a global one. In order to validate the performance of the MRIG metaheuristic, we first solve the homogeneous VRPMD and compare our results with the ones published in existing literature. Then, we extend the MRIG metaheuristic to solve the HeVRPMD. To solve this problem, we create a new set of instances based on the classical ones for the heterogeneous fleet vehicle routing

problem with unlimited driving ranges. The performance of the new metaheuristic is evaluated considering the distance-based costs and the green level of the fleet configurations. The green level of the fleet is measured by using two novel correlated green indexes. The first green index measures how green a fleet configuration is based on the fraction of 'green' vehicles in the fleet. The second green index directly computes the estimated environmental cost associated with the use of each vehicle in the fleet. The rest of the paper is organised as follows. First, we review the related literature in Section 2. Then, Section 3 provides the mathematical optimization model. The MRIG metaheuristic is described in Section 4. Section 5 presents the definition of the proposed green indexes and the computational experiments. The obtained results for the homogeneous case are analysed in Section 6, while the ones associated with the heterogeneous case are discussed in Section 7. Finally, some conclusions are provided in Section 8.

2 Literature review

The classical vehicle routing problem (VRP) and its variants have received extensive attention from practitioners and the research community (Laporte, 2009). While most VRP articles assume a fleet of homogeneous vehicles to serve the customers, in real-life it is usual to consider heterogeneous fleets of vehicles in terms of loading capacity (Koç et al., 2016; Dell'Amico et al., 2007; Dominguez et al., 2016). This section focuses on reviewing the following two streams of research: the green VRP and the VRP with a heterogeneous fleet of vehicles. The green VRP is a relatively recent variant of the VRP having the goal of reducing greenhouse gas emissions by considering alternative fuel-powered vehicle fleets, such as electricity (Erdoğan and Miller-Hooks, 2012). In addition to the reduction of the amount of gas emissions, the use of electricity imposes some restrictions, such as the limited driving-range autonomy. As a result, most of the electric VRP literature reports on alternative fuel stations to recharge the battery. In this context, Erdoğan and Miller-Hooks (2012); Schneider, Stenger and Goeke (2014) and Montoya et al. (2014) presented a green VRP considering alternative fuel stations to refill the tank or recharge the battery, while Jie et al. (2019) and Verma (2018) proposed another remedy to meet EVs' limited driving ranges . In these research papers, EVs should visit battery swapping stations to swap their batteries before their battery power runs out or their driving ranges terminate. Likewise, Lin, Zhou and Wolfson (2016) considered the vehicle load effect on the battery consumption while designing the optimal routing plan. Additionally, Keskin and Çatay (2016) included a partial recharging feature for electric VRP with time windows. This partial-recharging assumption has been included to make recharging times shorter. Also related to this research line, Felipe et al. (2014) proposed an electric VRP model which determines the amount of energy recharged and the technology used. A detailed review on the challenges of electric vehicles in logistics and transportation can be found in Juan et al. (2016).

The second stream of research addressed in this study is the heterogeneous VRP. As stated before, using a heterogeneous fleet of vehicles makes the model more realistic. In this regard, the use of hybrid fleets combining EVs, ICEVs, and PHEVs is a promising research area. Hiermann et al. (2016) and Vaz Penna et al. (2016) proposed an optimization problem combining the fleet size, mix VRP with time windows, and the use of EVs. The fleet size and mix VRP only cover conventional vehicles but they distinguish different types of vehicles according to their transportation capacity, battery size, and fixed cost. Goeke and Schneider (2015) incorporated an energy consumption model including speed, gradient, and cargo load distribution into a fleet size and mix VRP with time windows and the use of EVs. Despite the recent advances on EV-related technology and infrastructure, the development of recharging facilities throughout the road transportation networks might be only an option on the long run. Therefore, the travel range still remains as one of the main issues concerning the use of EVs in transportation activities. This issue has been addressed in Almouhanna et al. (2020), by discussing a location routing problem with constrained distance which is used EVs in the location and routing decisions. They developed a heuristic and a metaheuristic to minimize the total cost, which includes the opening cost of depots, the variable distance-based cost of vehicles, and the fixed cost of using vehicles. In Juan, Goentzel and Bektas (2014b), the authors addressed this issue by solving a VRP variant which considers a hybrid fleet of vehicles with multiple driving ranges and assume that all vehicles are homogeneous in terms of loading capacity. The use of multiple driving ranges is due to the fact that vehicles use different energy sources or even alternative battery types. These authors developed a Multi-Round Heuristic (MRH) that iteratively builds a solution for the problem. In Reyes-Rubiano et al. (2019), authors studied a VRP including homogeneous fleet of electric vehicles with a limited loading capacity and driving ranges and stochastic travel times. The authors proposed a simheuristic algorithm to design reliable routing plans in order to minimize the expected timebased cost required to complete the freight distribution plan.

A research stream related to the VRP with multiple driving ranges is the distance-constrained VRP. Few papers have studied the distance-constrained VRP. Among them, we can highlight the works of Kek, Cheu and Meng (2008), Li, Simchi-Levi and Desrochers (1992), and Laporte, Desrochers and Nobert (1984). In the context of alternative fuel-powered vehicle fleets, Erdoğan and Miller-Hooks (2012) developed a similar model to a distance-constrained VRP by considering a single driving range limitation on the tour duration. The VRP and its variants are NP-hard problems and different approaches, from exact methods to heuristics and metaheuristics, have been employed to solve them (Hokama, Miyazawa and Xavier, 2016; François et al., 2016; Andreatta et al., 2016). Soft computing based methods are very frequent when solving the VRP family of optimization problems. Authors of Brito et al. (2015) used fuzzy logic as a way of defining the constraints of the VRP optimization problem and made use of ant colony optimization as the solving strategy. Fuzzy logic was also used to define preference information of customers with respect to the satisfaction for a service time in a

multi-objective optimization problem using a solving strategy based on a genetic algorithm Ghannadpour et al. (2014). Genetic algorithms, both single- and multi-objective, have been widely used for VRPs and their variants. Karakatič and Podgorelec (2015) presented a complete review on the use of genetic algorithms for multi-depot VRPS. Recently, Pierre and Zakaria (2017) proposed a genetic algorithm with additional stochastic rules for a VRP with time windows and AbdAllah, Essam and Sarker (2017) presented an enhanced genetic algorithm that tries to increase both diversity and the capability to escape from local optima to solve a dynamic VRP in which not all customers are known in advance, but are revealed as the system progresses. The research developed in this paper extends previous work in two main directions. First, it proposes a new MRIG metaheuristic which outperforms the existing approaches for the homogeneous version of the problem – i.e., assuming that all vehicles have the same loading capacity. Secondly, it extends this MRIG metaheuristic so it can deal with the heterogeneous version of the problem too.

3 HeVRPMD optimization model

In this section, we describe the proposed HeVRPMD model, which considers a heterogeneous fleet of vehicles with respect to loading capacities as well as driving ranges. This VRP model can be seen as a combination of two distinct problems: (i) the VRP considering heterogeneous fleets of vehicles in terms of loading capacity Baldacci, Battarra and Vigo (2008); and (ii) the VRP with multiple driving ranges (VRPMD), where fleets are hybrid in terms of driving range but all vehicles are assumed to have the same loading capacity (Juan et al., 2014b). In the next subsections, we define the mathematical optimization model for the HeVRPMD. The proposed model aims to find alternative 'green' fleet configurations with minimum distance-based cost. The concept of green refers to the fact that we give priority to the use of small-size EVs over medium-size EVs, large-size ICEVs and PHEVs. In addition, as in many other vehicle routing problems, the following constraints need also to be fulfilled: (i) each route starts and ends at the depot, and it is associated with a vehicle type; (ii) each customer belongs to exactly one route; and (iii) loading capacities and driving ranges of the vehicles are never exceeded – notice that the considered vehicles are heterogeneous both in loading capacity and driving range.

A model representation of the HeVRPMD can be a directed graph $G = (N, A)$ consisting of a set N of $n+1$ nodes, $N = \{0, 1, \ldots, n\}$ and a set $A = \{(i, j) : i, j \in N, i \neq j\}$ which represents the arcs connecting pairs of nodes. Node 0 denotes the depot, where the vehicle fleets are located, and the remaining nodes represent the n customers. Each customer i has a known demand $q_i > 0$. We denote the distance-based cost associated with traveling from node i to node j by d_{ij}, with $d_{ij} = d_{ji} \geq 0$. In addition, there is a set K of k different types of vehicles, $K = \{1, 2, \ldots, k\}$. The number of vehicles for each type is assumed to be unlimited. Each vehicle of type l has a loading capacity Q^l as

well as a maximum driving range T^l. Three different decision variables are used in the model: (i) a binary decision variable x_{ij}^l, which takes the value of 1 if vehicle $l \in K$ travels from node i to j, and 0 otherwise; and (ii) two continuous decision variables u_i^l and v_i^l which represent the cumulative amount of load carried and distance traveled, respectively, by vehicle $l \in K$ when leaving customer $i \in N \backslash \{0\}$. The objective function is the minimization of total distance-based cost, subject to:

1. Satisfying all customers' demands.
2. Balancing of flows between nodes.
3. Loading capacity of vehicles.
4. Driving ranges of the vehicles.
5. Non-negativity and binary constraints.

To define the constraints we used the model provided by (Baldacci et al., 2008) to define the set of constraints related to items 1 to 3, and the model introduced by (Juan et al., 2014b) to define the set of constraints related to driving ranges of the vehicles. The objective function of the optimization model is defined in Equation 1. This function calculates the total distance-based cost of all used vehicles by adding the traveled distance by each vehicle l over all arcs $(i, j) \in A$:

$$Minimize\ z = \sum_{l \in K} \sum_{(i,j) \in A} d_{ij} x_{ij}^l \tag{1}$$

The constraints of the HeVRPMD model are defined from Equation 2 to 9. Equations 2 ensures that every customer is visited exactly once by a single vehicle:

$$\sum_{l \in K} \sum_{j \in N, i \neq j} x_{ij}^l = 1 \qquad \forall i \in N \backslash \{0\} \tag{2}$$

Equation 3 guarantees the flow conservation from and to a given customer node using a vehicle of type l. By doing so, a connection between node i and node $j \in N \backslash \{i\}$ is assured:

$$\sum_{j \in N, i \neq j} x_{ij}^l - \sum_{j \in N, i \neq j} x_{ji}^l = 0 \qquad \forall i \in N \backslash \{0\}, l \in K \tag{3}$$

Equations 4 and 5 ensure that the total load capacity of a vehicle type l on each tour does not exceed the vehicle capacity Q^l. More precisely, Equation 4 ensures that the load of the vehicle in the next node j depends on the load of the vehicle in the previous node i as well as on the demand of node j. As a result, the last node on a tour will denote the total amount of load carried by the vehicle:

$$u_i^l \leq u_j^l - q_j x_{ij}^l + Q^l (1 - x_{ij}^l) \qquad \forall l \in K, i \in N, j \in N \backslash \{0\}, i \neq j \tag{4}$$

Equation 5 ensures that load u_i^l is always greater than zero and less than the maximum capacity Q^l for a vehicle of type l:

$$0 \leq u_i^l \leq Q^l \qquad \forall l \in K, i \in N \backslash \{0\} \tag{5}$$

Constraints 6 and 7 guarantee that the total length of the route does not exceed the maximum range of vehicle l. Constraint 6 restricts the route travelled up to customer j (v_j) to be larger than the route travelled up to previous visited node i (v_i) plus the distance travelled between customer node i to customer j.

$$0 \leq v_i^l \leq v_j^l - d_{ij}x_{ij}^l + T^l(1 - x_{ij}^l) \qquad \forall l \in K, i \in N, j \in N \backslash \{0\}, i \neq j \tag{6}$$

Constraint 7 ensures that the current route travelled to be smaller than the maximum driving range of vehicle type $l \in K$ minus the route traveled between node $i \in N$ and node $j \in N$.

$$0 \leq v_i^l \leq T^l - d_{ij}x_{ij}^l \qquad \forall l \in K, \forall (i,j) \in N, i \neq j \tag{7}$$

Notice that constraints 4 to 7 in our model forbid sub-tours in the solution. In fact, similar constraints have been widely used in the VRP literature in order to eliminate sub-tours Erdoğan and Miller-Hooks (2012); Feillet (2010). Finally, Equations 8 and 9 guarantee the binary and non-negativity conditions of the decision variables:

$$x_{ij}^l \in 0,1 \qquad \forall l \in K, \forall (i,j) \in A \tag{8}$$

$$u_i^l, v_i^l \geq 0 \qquad \forall l \in K, \forall i \in N \backslash \{0\} \tag{9}$$

Even for small-scale instances of the homogeneous (simplified) version of this problem, it is not possible to obtain solutions in reasonable computing times using commercial optimization packages such as CPLEX. Therefore, in the remaining of this paper, we propose the use of a metaheuristic algorithm as the most effective way to deal with both the homogeneous and the heterogeneous versions.

4 The MRIG metaheuristic

This section describes the proposed MRIG metaheuristic to solve both the homogeneous VRPMD and its heterogeneous version. This algorithm is inspired by the successive approximations method proposed by Juan et al. (2014a) to solve the heterogeneous VRP. Accordingly, MRIG is a multi-round approach that solves the global heterogeneous VRP by dividing it into different homogeneous VRP. The main components of the algorithm are the construction of the initial solution, local improvement, and acceptance criterion. Each round of the MRIG approach consists of an optimization routing algorithm, run

inside an Iterated Greedy (IG) framework. At each round, the algorithm first selects a new subset of nodes and a new type of vehicles, thus defining a homogeneous fleet VRPMD. Then, the routing algorithm integrated into the IG framework searches for a near-optimal solution for the selected subset of nodes and vehicle type. Additionally, and in order to facilitate the generation of solutions with different fleet configurations, a penalty-based diversification mechanism is integrated within MRIG. This mechanism is applied after the construction of the initial solution and before the local improvement of the selected subset of nodes of the route. The penalty mechanism is applied for all the iterations of the algorithm and slightly modifies the initial driving range of each vehicle at random. This diversification technique has been extensively used in some metaheuristic approaches such tabu search and others. Mathematically, the penalty cost modifies the driving range of a vehicle of type l (T^l) to a new driving range value with random noise ($T^{l'}$), always with a variation below the 10% of the initial driving value of the vehicle.

The routing algorithm of the MRIG extends and enhances the popular Clarke and Wright's savings heuristic (Clarke and Wright, 1964), and the savings list of edges. One of the advantages of using this routing algorithm is that it does not require any complex parameter fine-tuning and is efficient to solve VRP, as reported in Quintero-Araujo et al. (2017); Ferone et al. (2019). Another important component of the MRIG is the heuristic. This heuristic is relatively simple, yet effective, which has obtained high-quality results in areas such as scheduling (Ruiz and Stützle, 2007), arc routing problems (González-Martín et al., 2012), and vehicle routing problems (Ruiz and Stützle, 2008; Chebbi and Chaouachi, 2015), among others. In a nutshell, it generates a sequence of promising solutions by iterating over greedy constructive heuristics using two main phases: destruction (some solution components are removed from a complete solution), and reconstruction (a greedy constructive heuristic is applied to reconstruct a complete solution). Once a candidate solution has been completed, an acceptance criterion decides whether or not the new constructed solution will replace the reference solution. Figure 1 shows a flowchart to illustrate the MRIG algorithm and its main components.

4.1 Construction of the initial candidate solution

The first step of the algorithm uses a multi-round process with a routing algorithm to obtain the initial solution. This routing algorithm is applied to each round of the process for each type of vehicle among the unused vehicles. This also means that assuming an unlimited fleet of vehicles of the same type and with the same loading capacity, a homogeneous VRPMD is solved for the nodes which are not yet served.

Thus, for example, a multi-round process will typically need three rounds to generate a global feasible solution when facing a problem with a fleet configuration composed of ICEs, PHEVs, and two types of EVs with two different battery capacities. The three rounds are associated with the unlimited range ICEs and PHEVs, medium range EVs with larger batteries, and short range EVs with smaller batteries, respectively. At each

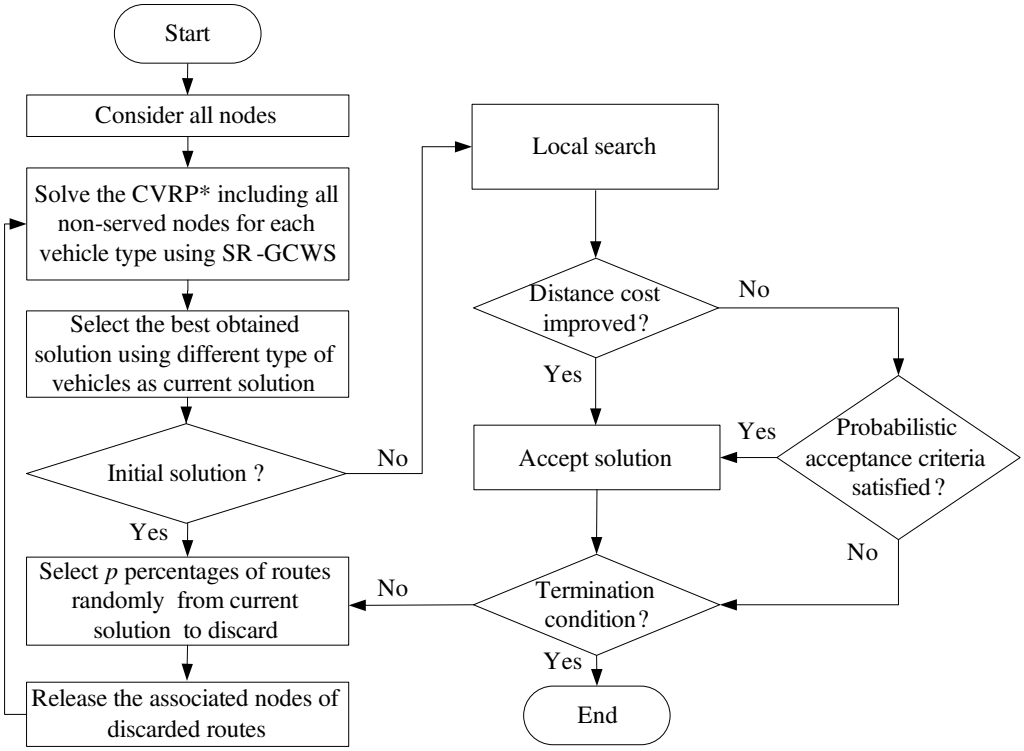

Figure 1: *Diagram of the multi-round algorithm to build the initial candidate solution.*

round of the solving method, a different homogeneous fleet capacitated VRP with a route length restrictions (CVRP*) is solved. The maximum route distance considered for each round is given by the maximum driving range of the corresponding unused vehicles. In the first round, when the problem specification includes unlimited driving-range vehicles (ICEs and PHEVs), no restriction is assumed on the route length, and the VRP is solved. In the remaining two rounds, when limited driving range vehicles are available, a CVRP* is solved considering the maximum route distance for the vehicles in this specific round (Belloso, Juan and Faulin, 2019). After solving the successive CVRP* with different types of vehicles and different driving ranges, the solution with the minimum distance-based cost is selected as the incumbent best solution. To produce the new solution, a ratio p of the routes of the current best solution are randomly selected to be discarded. The remaining $1-p$ routes are saved as partial solutions. The algorithm releases the associated nodes of the discarded routes and the same constructive process is used again to create the sub-solutions from these nodes which belong to the discarded routes. When all the nodes are served, the complete candidate solution, referred to as π_C, is built by merging the partial best sub-solutions obtained by the rounds of the algorithm. The process of the initial candidate solution construction is shown in Figure 2.

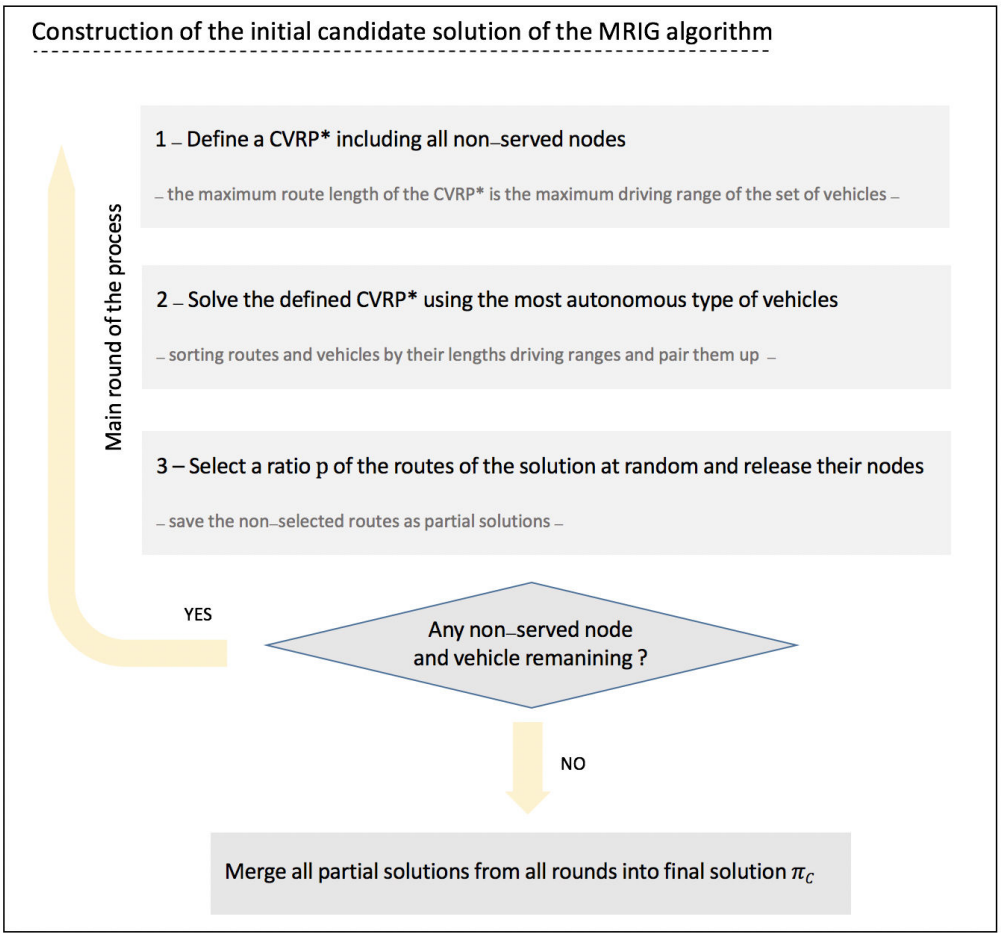

Figure 2: *Flowchart of the MRIG algorithm and its main components.*

4.2 Improvement phase

The second step of MRIG consists of two local search operators: destruction and reconstruction. The goal of this step is to improve the distance-based cost of the candidate solution, π_C. In the destruction phase, a sub-set of nodes, D, from the total n nodes is selected by using a ratio $d \in [0,1]$. This subset of nodes is removed from the routes and inserted into an archive list in the order they were selected. Note that, by following this process, there will not be any empty route (i.e., each route has at least one node). This destruction procedure explained in Algorithm 1, returns the list of removed nodes D as well as the list of routes containing the non-removed nodes. We denote τ_r to be the list of nodes assigned to route $r \in R$ of a candidate solution π_C.

During the construction phase, all the nodes of sub-set D are selected one by one according to the list order. Later, they are re-inserted into the existing routes. Among all

Algorithm 1 Destruction_$\pi_C(d)$

```
i ← 0
while i < ⌊dn⌋ do
   r ← Route randomly selected
   a ← Node randomly selected among the remaining nodes in the route r
   if |τ_r| > 1 then
      D ← Insert node a
      τ_r ← Remove node a from τ_r
      i ← i + 1
   end if
end while
return D and all τ_r, r ∈ R
```

the possible position, the chosen location for each node is the one in the route with the smallest distance-based cost. This process is repeated $\lfloor dn \rfloor$ times, until all the nodes of D are re-inserted, thus leaving D empty.

4.3 Acceptance criterion

Finally, MRIG uses an acceptance criterion that allows it to accept, from time to time, a degradation of the base solution. The criterion adds more diversity into the search and prevents the algorithm from getting stuck in a local optima. The acceptance criterion is applied once the improvement of the candidate solution, π_C, has been completed. Therefore, this step determines if the new generated solution should replace the base solution π_I even if it has a higher cost. The acceptance criterion of worse solutions is based on the probabilistic acceptance criterion of simulated annealing (Ruiz and Stützle, 2008; Yu and Lin, 2015; Wang et al., 2015). In MRIG, the acceptance criterion works as follows. Let $C_{(\pi_I)}$ denotes the distance-based cost of the current base solution π_I. The newly generated solution, π_C, is automatically accepted as the updated base solution if $C_{(\pi_C)} < C_{(\pi_I)}$. Otherwise, the solution π_C is accepted as an update of the base solution only if a certain criterion is met. This criterion relies on a probabilistic mechanism that takes into account the so-called temperature parameter and the change in the objective function value. It is defined in Equation 10, where *random* is a random number uniformly distributed between 0 and 1, and *Temp* is the temperature parameter originally proposed by Osman and Potts (1989):

$$random \leq e^{-\frac{C_{(\pi_C)} - C_{(\pi_I)}}{Temp}} \tag{10}$$

Hatami, Ruiz and Andrés-Romano (2015) simplified the latter acceptance mechanism by considering two aspects. First, they eliminated the *Temp* factor. Secondly, the probability of accepting a worse solution in the original mechanism of Equation 10 only depends on the difference between $C_{(\pi_C)}$ and $C_{(\pi_I)}$. This dependency provokes that the difference could be the same for instances with non-similar deterioration levels in terms of relative values. In order to solve this potential shortcoming, the difference, $C_{(\pi_C)} - C_{(\pi_I)}$,

is substituted by the Relative Percentage Difference (RPD) between the cost values of these two solutions. RPD value is obtained by $RPD(\pi_C, \pi_I) = \frac{C_{(\pi_C)} - C_{(\pi_I)}}{C_{(\pi_I)}} \times 100$. The improved criterion is simple and it does not need any parameter fine-tuning process. Therefore, we use it in the MRIG metaheuristic as shown in Equation 11.

$$random \leq e^{-RPD(\pi_C, \pi_I)} \tag{11}$$

5 Computational experiments

This section describes the experimental setup to evaluate the performance of MRIG. First, we describe how we evaluate the costs of the solutions (Section 5.1), as well as two new green indexes (Section 5.2). Secondly, Section 5.3 shows the benchmark instances used for the experiments.

5.1 Distance-based cost evaluation

Three types of vehicles are considered in the experiments: (i) large range ICEVs and PHEVs with no driving range limitations; (ii) medium range EVs, which have an autonomy of 200 distance units; and (iii) small range EVs, with an autonomy of 100 distance units. These three types of vehicles are denoted by L, M, and S, respectively. Accordingly, a fleet configuration for each problem instance is represented by $S/M/L$ (i.e., the number of vehicles of each type). In the computational experiments, the distance-based cost associated with the fleet configuration is computed. An analysis on how the substitution of ICEVs/PHEVs by EVs increases the distance-based cost is also provided.

5.2 Green indexes for fleet configurations

In order to compare the performance of MRIG with previous results from the literature, we have considered that one configuration is greener than another if: (i) it substitutes vehicles of type L by vehicles of type M or S, where S is always preferred over M; or (ii) vehicles of type M are substituted by vehicles of type S without increasing the number of vehicles of type L.

As mentioned before, vehicles of type S and M are EVs. It is assumed that a vehicle of type S has a lower driving range and a lower loading capacity than a vehicle of type M. A vehicle of type S can easily access high congested streets with limited parking space in many cities, and it is constrained to a lesser degree by the existence of traffic congestion or lack of parking areas than other larger-size vehicles (Juan et al., 2016). For these reasons, a vehicle of type S is considered greener than one of type M. In order to compare the green level of two different fleet configurations, we introduce two novel indexes. The first one, GI_1, is defined by Equation 12 and measures the fraction of S and M vehicles with respect to all vehicles in the fleet:

$$GI_1 = \frac{S + \omega M}{S + M + L} \tag{12}$$

where $\omega \in (0,1)$, and S, M, and L, denote the number of vehicles of each type. In the numerical experiments, we have set ω to 0.7, since the idea is that using a larger fraction of type M vehicles contributes to make the fleet greener, but not as much as using a larger fraction of vehicles of type S (considered to be the 'greenest' ones). Notice that this index will take the value of 0 whenever all the vehicles in the fleet are of type L (i.e., ICEVs or PHEVs), while it will take the value of 1 only when all the vehicles in the fleet are of type S (i.e., the greenest possible EVs). The second proposed index, GI_2, directly considers the environmental cost associated with using each type of vehicle. This index measures environmental unit cost for each fleet configuration. It is assumed that vehicles of type L have an associated cost of α monetary units. The environmental unit costs for vehicles of type M and S, which are less pollutant than type L, are set to β and γ, with $\alpha > \beta > \gamma > 0$. This index is defined by Equation 13. When applying this GI_2 index to a practical scenario, these cost values are required to be set based on additional data on the specific characteristics of each vehicle type. In our numerical experimentation we set $\alpha = 100$, $\beta = 30$, and $\gamma = 10$. These values are based on a preliminary experimentation where we tested different sets of values from the expert knowledge of a routing business collaborator. For example, in our experimental scenario, each vehicle of type L produces 10 times more environmental units than vehicles of type S; and each vehicle of type M is 3 times more pollutant than a vehicle of type S.

$$GI_2 = \gamma S + \beta M + \alpha L \tag{13}$$

These two green indexes offer alternative ways of measuring the degree of environment-friendly associated with a given fleet configuration. The idea here is that GI_1 can be used as a proxy for index GI_2 in those real-life situations in which estimating the exact values of α, β, and γ cannot be easily achieved due to the lack of accurate data. Figure 3 illustrates, for some of the solutions obtained in the numerical experiments which are discussed in the next section, the existence of a strong linear relationship between both indexes. Note that, in all the analysed instances, the determination coefficient is above 90%, which guarantees that – at least for the set of instances and numerical values considered in the experiments – GI_1 could be used to accurately estimate the value of GI_2, if necessary.

5.3 Problem instances and computing resources

We have used 33 classical VRP instances to validate our solving approach for both the VRPMD and HeVRPMD scenarios. These instances have been selected from a large set of instances available at `http://www.branchandcut.org`. The criteria we used to select these instances were to include those ones with detailed information on routes for the optimal or pseudo-optimal solution and having between 22 and 135 nodes. The charac-

teristics of these instances are also different among them (e.g., the number of nodes, the vehicle capacity, the location of the depot with respect to the clients, and their scattered or clustered topology). In addition, we need to set different loading capacities for the vehicles in the HeVRPMD scenario. To achieve this we assume that the fixed capacity in classical VRP instances, Q_0, corresponds to a vehicle of type M. Accordingly, the capacity associated with vehicles of types S and L is set to $0.8Q_0$ and $1.25Q_0$, respectively. MRIG was implemented using the Java programming language and run on an Intel® Core™i5 CPU M520 2.40GHz with 4GB RAM, and Windows 7 Pro as the operating system. The experimental results for each instance are obtained after 30 runs using different seeds for the random number generation. Our stopping criterion is the maximum CPU time, set to 300 seconds, which allows enough iterations for the metaheuristic to reach a good convergence for the majority of the instances. Finally, the p parameter of the initial solution construction is set to 0.6, while the d parameter of the destruction operator is set to 0.5. These values were obtained after a preliminary experimentation, according to the statistical learning methodology proposed in Calvet et al. (2016).

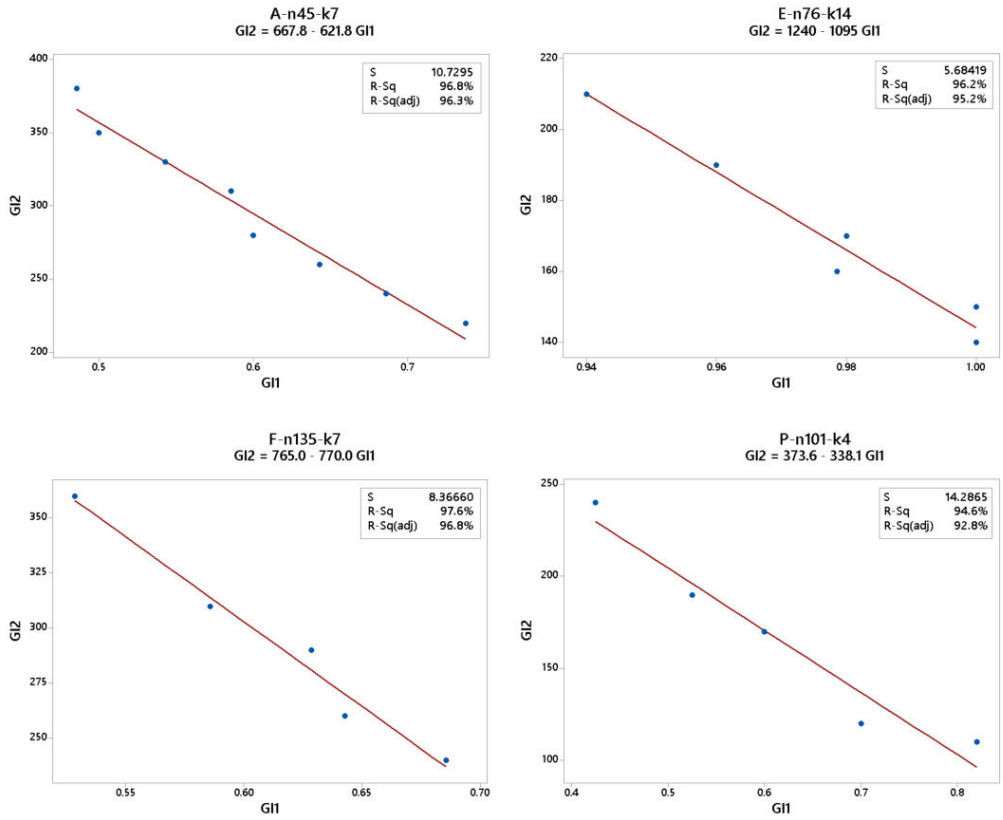

Figure 3: *Linear relationship between GI_1 and GI_2 for four problem instances.*

6 Analysis of results for the homogeneous VRPMD

To the best of our knowledge, the only algorithm considered in the literature to solve the homogeneous version of the VRPMD is the MRH one proposed in Juan et al. (2014b). The authors evaluated the performance of their MRH algorithm using 20 CVRP instances. In our paper, the number of instances tested has been increased up to 33, including the original 20 plus 13 additional ones. This allows us to directly compare the performance of our approach with the ones already published. The results are presented in Tables 1-3. These tables show the following information for each instance: its name, number of customers, vehicle capacity, and the distance-based cost of the best known solution (BKS) for the homogeneous VRP – without considering driving-range limitations – as provided in `http://www.branchandcut.org`. Also, these tables show a set of diverse feasible fleet configurations ($FleetCFG$) shown by $S/M/L$ those are found by the MRIG and MRH algorithms. For each instance, more than one feasible configuration has been found. However, only those solutions offering better values, either in distance-based cost or in green level, have been included in the tables. Notice that the "greener" configuration is considered. A configuration is greener than the other if it substitutes vehicles of type L by vehicles of type M or S (with S preferred over M), or vehicles of type M by vehicles of type S (without increasing the number of vehicles of type L). The associated distance-based cost for each fleet configuration, $DBCost$, is also included. The RPD column in each table shows the gap between the BKS and the distance-based costs provided by both algorithms. The best distance-based cost for each instance, and the associated gaps are indicated in bold. The last column of both tables shows the "diversified ratio", which is the ratio between the number of fleet configurations obtained using MRIG and MRH. Notice that, on the average, our MRIG provides 1.95 times more diversified fleet configurations than the MRH algorithm. In addition, the best distance-based cost obtained by MRIG is better than or equal to the one obtained by MRH in 80% of the instances.

Figure 4 illustrates the comparison using boxplots between three alternative solutions (A, B, and C) provided by both algorithms to show the gap differences with respect to the BKS of the problem. MRH-A and MRIG-A denote the best solution – in terms of distance-based cost – provided by each algorithm. Similarly, MRH-B and MRIG-B refer to alternative solutions that are greener than the previous ones. Finally, MRH-C and MRIG-C are solutions even greener than the ones provided by configuration B. Notice that solutions A provided by algorithms MRH and MRIG perform quite well in terms of their associated distance-based costs, since they offer very low gaps with respect to the BKS for the classical VRP – which is not considering any range constraint. As expected, the distance-based-cost gap with respect to the BKS increases as greener fleet configurations (suffixes B and C) are used. However, the average gap associated to MRIG is noticeably lower than the one associated to MRH for both B and C alternative configurations.

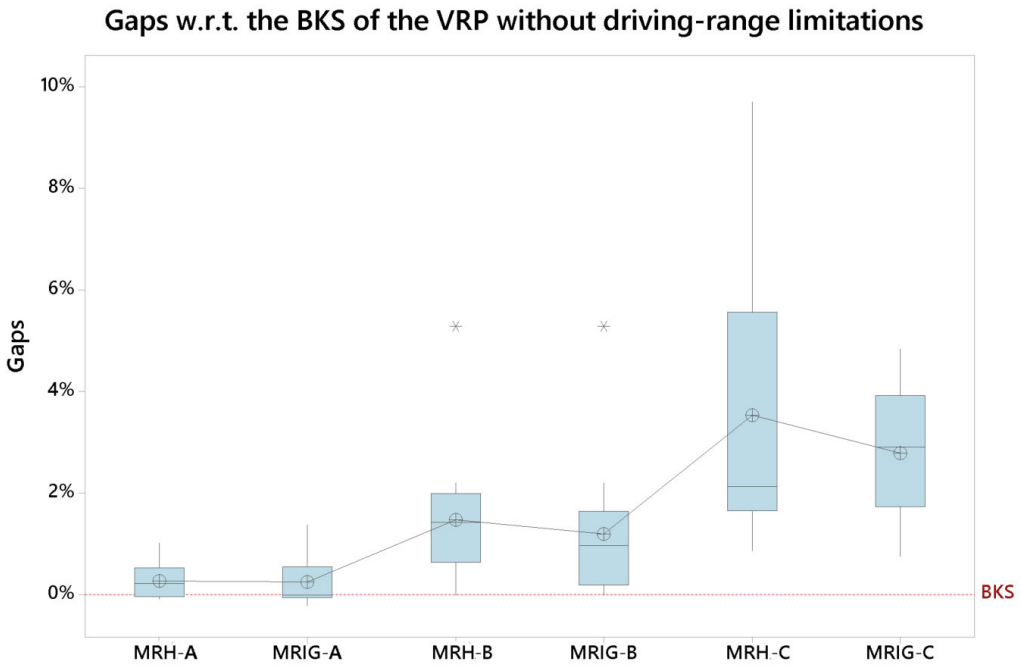

Figure 4: *Visual comparison using boxplots of three alternative solutions (A, B, and C) found by MRIG and MRH.*

Being able to select among different fleet configurations enriches the decision-making process. Thus, for example, the set of fleet configurations found by MRIG are more diversified and greener than those found by MRH in instance F-n135-k7. Moreover, MRIG can solve the instance using less vehicles of type L (ICEVs or PHEVs), since these are substituted by vehicles of types S and M (small- and medium-range EVs). Likewise, for the same fleet configuration, MRIG can find routes with a lower distance-based cost. For example, the greenest fleet configuration obtained by MRH is $3/2/2$, i.e.: it includes 3 vehicles of type S, 2 vehicles of type M, and 2 vehicles of type L. The associated distance-based cost is 1,190.07. For the same instance, MRIG was able to find a solution with an associated distance-based cost of 1,175.68 using the same fleet configuration. Furthermore, MRIG could find greener fleet configurations, such as $1/5/1$ and $2/4/1$, where the number of type L vehicles is decreased even further.

Table 1: *Experimental results for 20 classical VRP instances*

Instance name	Number of nodes	Capacity	*BKS*	*MRH*		*MRIG*		*RPD*		Diversified Ratio
				Fleet $CFG.$ $S/M/L$	*DBCost*	Fleet $CFG.$ $S/M/L$	*DBCost*	*MRH*	*MRIG*	
A-n32-k5	32	100	787.81	2/1/2	**787.08**	2/1/2	**787.08**	**0.00**	**0.00**	1
				1/3/1	829.41	1/3/1	829.41	5.38	5,38	
A-n38-k5	38	100	734.18	0/5/0	**733.95**	0/5/0	**733.95**	**0.00**	**0.00**	1.25
				1/3/1	734.18	1/3/1	734.18	0.03	0,03	
				1/4/0	735.05	1/4/0	735.05	0.15	0,15	
				3/3/0	763.13	3/3/0	755.89	3.97	2,99	
						1/5/0	**733.95**	-	-	
A-n65-k9	65	100	1181.69	1/8/0	**1183.31**	1/8/0	**1181.69**	**0.14**	**0.00**	1
				2/7/0	1191.27	2/7/0	1188.03	0.81	0.54	
				5/5/0	1276.21	5/5/0	1280.81	8.00	8.39	
				3/6/1	1238.33	3/6/1	1226.60	4.79	3.80	
				4/6/0	1253.81	4/6/0	1230.52	6.10	4.13	
				3/5/1	1297.31	3/6/0	1233.86	-	-	
A-n80-k10	80	100	1766.50	2/5/3	**1776.19**	2/5/3	**1775.75**	**0.55**	**0.52**	2.5
				1/7/2	1785.05	1/7/2	1785.04	1.05	1.05	
						2/6/2	1794.42	-	-	
						0/9/1	1994.16	-	-	
						2/8/1	2016.21	-	-	
B-n50-k7	50	100	744.78	2/5/0	**744.23**	2/5/0	**744.23**	**0.00**	**0.00**	1.67
				3/4/0	744.67	3/4/0	744.67	0.06	0.06	
				4/3/0	751.24	4/3/0	750.42	0.94	0.83	
						5/2/0	785.01	-	-	
						6/1/1	836.38	-	-	
B-n52-k7	52	100	750.08	4/2/1	**752.63**	4/2/1	**750.03**	**0.35**	**0.00**	1.5
				3/4/0	756.71	3/4/0	756.71	0.89	0.89	
						5/0/3	899.58	-	-	
B-n57-k9	57	100	1603.63	0/4/5	**1602.29**	0/4/5	**1602.29**	**0.00**	**0.00**	1.6
				0/5/4	1603.37	0/5/4	1603.37	0.07	0.07	
				0/6/3	1631.66	0/6/3	1631.85	1.83	1.84	
				1/3/5	1642.53	1/3/5	1636.34	2.51	2.13	
				1/4/4	1646.65	1/4/4	1637.44	2.77	2.19	
						1/5/3	1650.87	-	-	
						2/2/6	1694.09	-	-	
						0/7/2	1707.81	-	-	
B-n78-k10	78	100	1229.27	4/6/0	1253.10	4/6/0	**1245.64**	1.94	**1.33**	0.6
				6/5/0	1292.60	6/5/0	1288.67	5.15	4.83	
				3/7/0	1251.83	3/7/0	1246.21	1.84	1.38	
				4/5/1	**1236.33**			**0.57**	-	
				4/4/2	1252.76			-	-	
E-n22-k4	22	6000	375.28	2/2/0	**375.28**	2/2/0	**375.28**	**0.00**	**0.00**	2
				3/1/0	383.52	3/1/0	383.52	2.20	2.20	
						1/3/0	386.03	-	-	
						6/0/0	519.13	-	-	
E-n30-k3	30	4500	535.80	1/3/0	**505.01**	1/3/0	**505.01**	**0.00**	**0.00**	4
						2/1/1	579.78	-	-	
						3/0/2	597.65	-	-	
						3/1/1	633.37	-	-	

***Table 2**: Continued - Experimental results for 20 classical VRP instances*

Instance name	Number of nodes	Capacity	*BKS*	*MRH*		*MRIG*		*RPD*		Diversified Ratio
				Fleet $CFG.$ $S/M/L$	*DBCost*	Fleet $CFG.$ $S/M/L$	*DBCost*	*MRH*	*MRIG*	
E-n51-k5	51	160	524.94	3/2/0	**524.63**	3/2/0	**524.61**	**0.00**	**0.00**	3
						5/1/0	556.92	-	-	
						6/0/0	578.01	-	-	
E-n76-k10	76	140	837.36	7/3/0	**845.80**	7/3/0	**842.57**	**1.01**	**0.62**	4
				8/2/0	856.70	8/2/0	848.73	2.31	1.36	
				11/0/0	854.42	9/1/0	864.70	-	-	
						10/0/0	879.88	-	-	
E-n76-k14	76	100	1026.71	13/2/0	**1031.94**	13/2/0	1043.48	**0.51**	1.63	1.5
				14/1/0	1041.58	14/1/0	1044.28	1.45	1.71	
				13/1/0	1043.29	13/1/0	1060.05	1.61	3.25	
				15/0/0	1045.77	15/0/0	1050,79	1.86	2.35	
						12/3/0	**1038.48**		**1.15**	
						14/0/0	1075.74	-	-	
F-n135-k7	135	2210	1170.65	3/1/3	**1175.73**	3/1/3	**1168.01**	**0.66**	**0.00**	2.5
				3/2/2	1190.07	3/2/2	1175.68	1.89	0.66	
						2/3/2	1171.18	-	-	
						1/5/1	1215.14	-	-	
						2/4/1	1241.70	-	-	
M-n101-k10	101	200	819.81	8/2/0	**821.11**	8/2/0	**819.56**	**0.19**	**0.00**	3
						9/1/0	847.42	-	-	
						10/1/0	868.31	-	-	
M-n121-k7	121	200	1045.16	2/3/2	**1047.96**	2/3/2	**1044.64**	**0.32**	**0.00**	2
				1/7/0	1274.60	1/7/0	1287.52	22.01	23.25	
						3/2/3	1050.66	-	-	
						1/5/1	1129.40	-	-	
P-n50-k10	50	100	699.56	10/0/0	**700.66**	10/0/0	**700.66**	**0.16**	**0.16**	1
P-n55-k15	55	70	991.48	16/0/0	**952.02**	16/0/0	**953.18**	**0.00**	**0.12**	1
P-n70-k10	70	135	830.02	8/2/0	**834.38**	8/2/0	843.63	**0.53**	1.64	2.5
				10/0/0	841.56	10/0/0	851.39	1.39	2.57	
						6/4/0	**841.42**	-	**1.37**	
						9/1/0	844.35	-	-	
						7/3/0	842.36	-	-	
P-n76-k5	76	280	635.04	1/4/0	**638.44**	1/4/0	636.40	**0.55**	0.23	1.3
				2/3/0	647.51	2/3/0	653.07	1.97	2.85	
				4/2/0	696.63	4/2/0	666.60	9.71	4.98	
						0/5/0	**634.97**	-	**0.00**	
Average								2.08	1.92	1.95
								0.28	**0.26**	

Table 3: *Experimental results for 13 additional VRP instances*

Instance name	Number of nodes	Capacity	*BKS*	*MRIG*		RPD
				Fleet $CFG.\ S/M/L$	Cost	
A-n45-k7	45	100	1147.28	2/2/3	1146.77	0.00
				1/4/2	1154.43	0.67
				2/3/2	1155.60	0.77
				1/5/1	1191.29	3.88
				0/5/2	1174.01	2.38
				0/6/1	1230.27	7.28
				1/7/0	1463.93	27.66
				2/4/1	1186.46	3.46
A-n55-k9	55	100	1074.46	3/6/0	1074.46	0.00
				4/5/0	1092.88	1.71
				6/4/0	1150.04	7.03
A-n60-k9	60	100	1355.8	2/6/1	1357.72	0.14
A-n61-k9	61	100	1039.08	4/6/0	1040.31	0.12
				5/5/0	1045.40	0.61
				6/4/0	1057.00	1.72
				7/3/0	1091.31	5.03
E-n33-k4	33	8000	838.72	0/2/2	837.67	0.00
				0/3/1	847.37	1.16
E-n76-k7	76	220	687.60	3/4/0	690.20	0.38
				4/3/0	695.26	1.11
				5/2/0	705.97	2.67
				6/1/0	733.74	6.71
F-n45-k4	45	2010	724.57	1/2/1	723.54	0.00
				2/0/2	792.37	9.51
F-n72-k4	72	30000	248.81	4/0/0	241.97	0.00
P-n22-k8	22	3000	601.42	8/1/0	588.79	0.00
				9/0/0	647.63	9.99
P-n40-k5	40	140	461.73	5/0/0	461.73	0.00
P-n65-k10	65	130	796.67	10/0/0	797.82	0.14
P-n76-k4	76	350	598.22	0/4/0	600.55	0.39
				1/3/0	618.53	3.40
P-n101-k4	101	400	692.28	0/3/1	691.29	0.00
				0/4/0	694.67	0.49
				1/1/2	703.91	1.83
				1/2/1	700.88	1.39
				2/3/0	729.90	5.59

Regarding the 13 new instances analysed in this work, the results obtained with our MRIG approach are provided in Table 3. Notice that even considering the driving-range limitation, the distance-based cost of the best solution provided by the MRIG in 300 seconds is always similar to the classical BKS for the unconstrained problem. In other words, using an algorithm such as MRIG, it is frequently possible to find alternative solutions for the VRPMD with greener fleet configurations while, at the same time, these

solutions offer reasonably low distance-based costs – i.e., similar to the best ones that can be obtained for the classical VRP without driving-range limitations. Table 3 also shows that, in 9 out of 13 instances, the MRIG algorithm was able to generate alternative solutions with greener fleet configurations using less large vehicles. Even in these cases, the associated distance-based costs obtained by our algorithm are reasonably low. All in all, this section has shown that our algorithm is able to outperform the previous existing one for solving the homogeneous version of the VRPMD, both in terms of distance-based cost as well as in terms of green level of the solutions. Also, from a managerial perspective, the message is clear: (i) the introduction of EVs – with limited driving range – in transportation fleets does not have to cause a significant increase in distance-based costs (at least as far as an intelligent algorithm is used to optimize the associated routing problem); and (ii) among the different routing plans that such an algorithm can generate in just a few minutes, it is usually possible to choose one that offers a low distance-based cost while, at the same time, employs less contaminant vehicles. Despite the clear advantages of our approach, being a metaheuristic algorithm it cannot guarantee the optimality of the best-found solution. In addition, there is not a unique way of measuring the green level of a routing solution, since this is still a controversial concept in the scientific literature Juan et al. (2016).

7 Analysis of results for the heterogeneous HeVRPMD

The proposed algorithm is not only able to outperform the state-of-the-art results for the homogeneous VRPMD, but it can also solve the realistic heterogeneous version of the problem (i.e., HeVRPMD). Tables 4 to 6 show the results obtained by the algorithm when solving the HeVRPMD problem. These tables show the instance name and loading capacity in the homogeneous case Q_0 (first column), the best known solution (BKS) for the classical VRP without driving range limitations (second column), and loading capacities VS-VM-VL for small, medium, and large vehicles, respectively (third column). As stated in Section 5.3, heterogeneous instances were generated by considering $VS = 0.8Q_0$, $VM = Q_0$, and $VL = 1.25Q_0$. The MRIG algorithm provides, for each heterogeneous instance, a set of solutions. The solution with the minimum distance-based cost (*DBCost*) found by the MRIG is shown in bold and therefore, its corresponding *RPD* value is 0. Apart from the solution with the minimum *DBCost*, two sets of three solutions each are shown ($SetGI_1$ and $SetGI_2$). These three different fleet configurations are shown based on the minimum, medium, and maximum number of large vehicles, noted by L_s, L_m, and L_l, respectively. Green indexes GI_1 and GI_2 are shown for all the solutions (sixth and seventh columns for those of $SetGI_1$ and, 11-th and 12-th columns for those of $SetGI_2$). Therefore, Tables 4 to 6 report between six or seven solutions for each instance, depending on the case the minimum *DBCost* solution also belongs to the set of "green" solutions. At the end of Table 6, the average *RPD* values are also shown. About 42% of the solutions provided by MRIG reach the maximum green level

Table 4: *Experimental results for the HeVRPMD.*

Instance name (Q_0)	BKS Cost	VS-VM-VL	$SetGI_1$					$SetGI_2$				
			Fleet CFG. S/M/L	*DBCost*	GI_1	GI_2	*RPD*	Fleet CFG. S/M/L	*DBCost*	GI_1	GI_2	*RPD*
A-n32-k5(100)	787.81	80-100-125	**1/0/3**	**687.58**	0.25	310	**0.00**					
			0/0/4^{L_s}	730.19	0.00	400	6.20	0/0/5^{L_s}	1151.57	0.00	500	67.48
			1/1/2^{L_m}	695.44	0.43	240	1.14	1/1/3^{L_m}	726.91	0.34	340	5.72
			4/2/1^{L_l}	830.40	0.77	200	20.77	2/2/1^{L_l}	738.58	0.68	180	7.42
A-n38-k5(100)	734.18	80-100-125	**0/0/4**^{L_s}	**644.25**	0.00	400	**0.00**	0/1/5^{L_s}	1235.46	0.12	530	91.77
			2/1/3^{L_m}	672.16	0.45	350	4.33	2/0/3^{L_m}	676.67	0.40	320	5.03
			6/3/0^{L_l}	903.39	0.90	150	40.22	3/3/0^{L_l}	780.15	0.85	120	21.09
A-n45-k7(100)	1147.28	80-100-125	**1/0/5**	**990.18**	0.17	510	**0.00**					
			0/0/6^{L_s}	1079.11	0.00	600	8.98	1/1/7^{L_s}	1663.92	0.19	740	68.04
			3/1/5^{L_m}	1167.23	0.41	560	17.88	2/2/4^{L_m}	1100.33	0.43	480	11.12
			5/7/0^{L_l}	1675.26	0.83	260	69.19	1/7/0^{L_l}	1459.94	0.74	220	47.44
A-n55-k9(100)	1074.46	80-100-125	**0/0/7**^{L_s}	**942.84**	0.00	700	**0.00**	1/0/8^{L_s}	1326.54	0.11	810	40.70
			4/0/6^{L_m}	1014.94	0.40	640	7.65	1/3/4^{L_m}	968.22	0.39	500	2.69
			8/4/0^{L_l}	1272.33	0.90	200	34.95	8/4/0^{L_l}	1272.33	0.90	200	34.95
A-n60-k9(100)	1355.8	80-100-125	**0/1/6**	**1153.56**	0.10	630	**0.00**					
			0/0/7^{L_s}	1164.19	0.00	700	0.92	0/1/8^{L_s}	1697.11	0.08	830	47.12
			2/2/5^{L_m}	1184.15	0.38	580	2.65	1/2/5^{L_m}	1175.03	0.30	570	1.86
			5/6/1^{L_l}	1422.37	0.77	330	23.30	2/6/1^{L_l}	1334.07	0.69	300	15.65
A-n61-k9(100)	1039.08	80-100-125	**1/0/7**	**909.60**	0.13	710	**0.00**					
			0/0/8^{L_s}	935.72	0.00	800	2.87	2/0/8^{L_s}	1323.97	0.20	820	45.55
			4/1/5^{L_m}	965.43	0.47	570	6.14	4/2/4^{L_m}	988.82	0.54	500	8.71
			11/3/0^{L_l}	1311.24	0.94	200	44.15	9/3/0^{L_l}	1230.46	0.93	180	35.27
A-n65-k9(100)	1181.69	80-100-125	**1/0/7**	**1051.34**	0.13	710	**0.00**					
			0/0/8^{L_s}	1068.09	0.00	800	1.59	1/1/8^{L_s}	1604.55	0.17	840	52.62
			4/0/5^{L_m}	1142.82	0.44	540	8.70	1/4/4^{L_m}	1081.21	0.42	530	2.84
			8/5/0^{L_l}	1464.39	0.88	230	39.29	7/5/0^{L_l}	1398.35	0.88	220	33.01
A-n80-k10(100	1766.5	80-100-125	**0/1/7**	**1511.77**	0.09	730	**0.00**					
			0/0/8^{L_s}	1516.03	0.00	800	0.28	0/0/10^{L_s}	2368.14	0.00	1000	56.65
			4/0/7^{L_m}	1674.59	0.36	740	10.77	1/2/6^{L_m}	1533.72	0.27	670	1.45
			3/8/1^{L_l}	1948.24	0.72	370	28.87	1/8/1^{L_l}	1857.37	0.66	350	22.86
B-n50-k7(100)	744.78	80-100-125	**2/0/4**	**615.88**	0.33	420	**0.00**					
			0/0/5^{L_s}	619.18	0.00	500	0.54	1/0/6^{L_s}	952.27	0.14	610	54.62
			0/4/2^{L_m}	643.47	0.47	320	4.48	1/2/3^{L_m}	623.59	0.40	370	1.25
			9/2/0^{L_l}	950.75	0.95	150	54.37	7/2/0^{L_l}	848.22	0.93	130	37.73
B-n52-k7(100)	750.08	80-100-125	**0/0/5**^{L_s}	**650.00**	0.00	500	**0.00**	1/0/6^{L_s}	948.90	0.14	610	45.98
			3/0/4^{L_m}	686.33	0.43	430	5.59	2/2/3^{L_m}	662.08	0.49	380	1.86
			5/4/0^{L_l}	802.93	0.87	170	23.53	3/4/0^{L_l}	773.18	0.83	150	18.95
B-n57-k9(100)	1603.63	80-100-125	**0/0/7**^{L_s}	**1317.27**	0.00	700	**0.00**	0/0/9^{L_s}	2183.29	0.00	900	65.74
			2/1/6^{L_m}	1337.82	0.30	650	1.56	1/1/6^{L_m}	1324.36	0.21	640	0.54
			1/9/2^{L_l}	2013.19	0.61	480	52.83	0/6/2^{L_l}	1565.40	0.53	380	18,84
B-n78-k10(100)	1229.27	80-100-125	**0/0/8**^{L_s}	**1048.11**	0.00	800	**0.00**	0/1/9^{L_s}	1718.67	0.07	930	63.98
			4/1/6^{L_m}	1124.33	0.43	670	7.27	2/2/5^{L_m}	1066.13	0.38	580	1.72
			6/6/0^{L_l}	1327.24	0.85	240	26.63	6/6/0^{L_l}	1327.24	0.85	240	26.63
E-n22-k4(6000)	375.28	4800-6000-7500	**1/1/2**	**369.19**	0.43	240	**0.00**					
			0/0/3^{L_s}	377.68	0.00	300	2.30	1/1/3^{L_s}	439.38	0.34	340	19.01
			2/0/2^{L_m}	376.90	0.50	220	2.09	1/3/1^{L_m}	373.37	0.62	200	1.13
			6/0/0^{L_l}	533.15	1.00	60	44.41	6/0/0^{L_l}	533.15	1.00	60	44.41

Table 5: *Continued - Experimental results for the HeVRPMD.*

Instance name (Q_0)	BKS Cost	VS-VM-VL	$SetGI_1$					$SetGI_2$				
			Fleet CFG. S/M/L	*DBCost*	GI_1	GI_2	*RPD*	Fleet CFG. S/M/L	*DBCost*	GI_1	GI_2	*RPD*
E-n30-k3 (4500)	535.8	3600-4500-5625	**0/1/2**	**477.66**	0.23	230	**0.00**					
			0/0/3^{L_s}	507.64	0.00	300	6.28	1/0/4^{L_s}	922.54	0.20	410	93.14
			1/1/2^{L_m}	480.54	0.43	240	0.60	2/1/2^{L_m}	480.54	0.54	250	0.60
			3/3/0^{L_l}	507.17	0.85	120	6.18	0/3/0^{L_l}	550.91	0.70	90	15.33
E-n33-k4(8000)	838.72	6400-8000-10000	**0/0/3^{L_s}**	**704.32**	0.00	300	**0.00**	1/0/4^{L_s}	930.78	0.20	410	32.15
			1/2/3^{L_m}	856.47	0.40	370	21.60	**0/0/3^{L_m}**	**704.32**	0.00	300	**0.00**
			2/3/1^{L_l}	998.74	0.68	210	41.80	0/3/1^{L_l}	829.35	0.53	190	17.75
E-n51-k5(160)	524.94	128-160-200	**0/0/4^{L_s}**	**497.74**	0.00	400	**0.00**	1/1/4^{L_s}	656.74	0.28	440	31.94
			3/0/3^{L_m}	522.59	0.50	330	4.99	2/1/2^{L_m}	520.60	0.54	250	4.59
			7/0/0^{L_l}	598.69	1.00	70	20.28	7/0/0^{L_l}	598.69	1.00	70	20.28
E-n76-k7(220)	687.60	176-220-275	**1/0/5**	**648.07**	0.17	510	**0.00**					
			0/0/6^{L_s}	1083.78	0.00	600	67.23	0/0/6^{L_s}	1083.78	0.00	600	67.23
			4/0/4^{L_m}	695.36	0.50	440	7.30	2/1/3^{L_m}	667.59	0.40	350	3.01
			9/0/0^{L_l}	791.22	1.00	90	22.09	9/0/0^{L_l}	791.22	1.00	90	22.09
E-n76-k10(140)	837.36	112-140-175	**0/0/8^{L_s}**	**757.81**	0.00	800	**0.00**	1/1/8^{L_s}	903.53	0.17	840	19.23
			5/0/5^{L_m}	824.65	0.50	550	8.82	1/6/3^{L_m}	819.66	0.52	490	8.16
			18/0/0^{L_l}	1235.73	1.00	180	63.07	13/0/0^{L_l}	986.11	1.00	130	30.13
E-n76-k14(100)	1026.71	80-100-125	**1/0/11**	**902.69**	0.08	1110	**0.00**					
			0/0/12^{L_l}	930.71	0.00	1200	3.10	18/0/0^{L_s}	1251.03	1.00	180	38.59
			8/0/8^{L_m}	990.48	0.50	880	9.73	4/5/5^{L_m}	988.25	0.54	690	9.48
			19/0/0^{L_s}	1238.74	1.00	190	37.23	1/0/12^{L_l}	946.84	0.08	1210	4.89
F-n45-k4 (2010)	724.57	1608-2010-2512	**0/0/3^{L_s}**	**690.89**	0.00	300	**0.00**	2/0/4^{L_s}	1126.57	0.33	420	63.06
			2/0/3^{L_m}	714.90	0.40	320	3.48	0/3/2^{L_m}	810.13	0.42	290	17.26
			4/2/1^{L_l}	744.86	0.77	200	7.81	3/1/1^{L_l}	860.73	0.74	160	24.58
F-n72-k4(30000)	248.81	24000-30000-37500	**0/3/1**	**237.53**	0.53	190	**0.00**					
			1/0/3^{L_s}	242.82	0.25	310	2.23	3/0/3^{L_s}	269.56	0.50	330	13.48
			2/0/3^{L_m}	250.35	0.40	320	5.40	**0/3/1^{L_m}**	**237.53**	0.53	190	**0.00**
			5/0/0^{L_l}	270.60	1.00	50	13.92	5/0/0^{L_l}	270.60	1.00	50	13.92
F-n135-k7(2210)	1170.65	1768-2210-2762	**1/0/5**	**1053.07**	0.17	510	**0.00**					
			0/0/6^{L_s}	1070.75	0.00	600	1.68	2/0/7^{L_s}	1838.11	0.22	720	74.55
			4/0/5^{L_m}	1206.49	0.44	540	14.57	1/2/4^{L_m}	1071.17	0.34	470	1.72
			10/2/1^{L_l}	1455.24	0.83	260	38.19	4/3/1^{L_l}	1217.92	0.76	230	15.65
M-n101-k10(200)	819.81	60-200-250	**1/0/7**	**757.61**	0.13	710	**0.00**					
			0/0/8^{L_s}	787.39	0.00	800	3.93	0/0/8^{L_s}	787.39	0.00	800	3.93
			4/2/5^{L_m}	861.15	0.49	600	13.67	4/1/4^{L_m}	790.40	0.52	470	4.33
			14/1/0^{L_l}	1122.67	0.98	170	48.19	11/1/0^{L_l}	1014.53	0.98	140	33.91
M-n121-k7(200)	1045.16	60-200-250	**1/0/5**	**953.34**	0.17	510	**0.00**					
			0/0/6^{L_s}	965.17	0.00	600	1.24	3/0/7^{L_s}	1680.06	0.30	730	76.23
			4/0/6^{L_m}	1537.13	0.40	640	61.24	1/2/4^{L_m}	967.07	0.34	470	1.44
			4/7/0^{L_l}	1393.23	0.81	250	46.14	1/7/0^{L_l}	1289.11	0.74	220	35.22
P-n22-k8(3000)	601.42	2400-3000-3750	**1/1/5**	**507.16**	0.24	540	**0.00**					
			0/0/7^{L_s}	524.97	0.00	700	3.51	0/0/7^{L_s}	524.97	0.00	700	3.51
			3/2/4^{L_m}	536.91	0.49	490	5.87	2/3/3^{L_m}	541.46	0.51	410	6.76
			14/1/0^{L_l}	876.21	0.98	170	72.77	10/1/0^{L_l}	783.15	0.97	130	54.42

Table 6: *Continued - Experimental results for the HeVRPMD.*

Instance name (Q_0)	BKS Cost	VS-VM-VL	$SetGI_1$					$SetGI_2$				
			Fleet CFG. S/M/L	*DBCost*	GI_1	GI_2	*RPD*	Fleet CFG. S/M/L	*DBCost*	GI_1	GI_2	*RPD*
P-n40-k5(140)	461.73	112-140-175	**0/1/3**	**431.67**	0.18	330	**0.00**					
			$0/0/4^{L_s}$	432.23	0.00	400	0.13	$2/0/4^{L_s}$	584.80	0.33	420	35.47
			$3/0/3^{L_m}$	457.78	0.50	330	6.05	$4/0/2^{L_m}$	463.83	0.67	240	7.45
			$6/0/0^{L_l}$	514.97	1.00	60	19.30	$6/0/0^{L_l}$	514.97	1.00	60	19.30
P-n50-k10(100)	699.56	80-100-125	$\mathbf{0/0/8^{L_s}}$	**607.39**	0.00	800	**0.00**	$0/1/8^{L_s}$	658.36	0.08	830	8.39
			$5/0/5^{L_m}$	669.00	0.50	550	10.14	$0/6/3^{L_m}$	657.15	0.47	480	8.19
			$13/0/0^{L_l}$	805.71	1.00	130	32.65	$13/0/0^{L_l}$	805.71	1.00	130	32.65
P-n55-k15(70)	991.48	56-70-87	$\mathbf{0/0/13^{L_s}}$	**824.21**	0.00	1300	**0.00**	$0/1/13^{L_s}$	883.51	0.05	1330	7.20
			$8/0/8^{L_m}$	915.58	0.50	880	11.09	$3/8/4^{L_m}$	919.94	0.57	670	11.62
			$20/0/0^{L_l}$	1126.70	1.00	200	36.70	$20/0/0^{L_l}$	1126.70	1.00	200	36.70
P-n65-k10(130)	796.67	104-130-162	$\mathbf{0/0/8^{L_s}}$	**726.51**	0.00	800	**0.00**	$3/0/8^{L_s}$	831.83	0.27	830	14.50
			$5/0/5^{L_m}$	779.95	0.50	550	7.36	$0/6/3^{L_m}$	766.30	0.47	480	5.48
			$13/0/0^{L_l}$	931.96	1.00	130	28.28	$13/0/0^{L_l}$	931.96	1.00	130	28.28
P-n70-k10(135)	830.02	108-135-196	$\mathbf{0/0/8^{L_s}}$	**760.93**	0.00	800	**0.00**	$1/1/8^{L_s}$	916.60	0.17	840	20.46
			$5/0/5^{L_m}$	821.68	0.50	550	7.98	$1/6/3^{L_m}$	812.82	0.52	490	6.82
			$13/0/0^{L_l}$	969.13	1.00	130	27.36	$13/0/0^{L_l}$	969.13	1.00	130	27.36
P-n76-k4(350)	598.22	280-350-437	**1/1/2**	**594.64**	0.43	240	**0.00**					
			$0/0/4^{L_s}$	695.78	0.00	400	17.01	$2/1/4^{L_s}$	935.17	0.39	450	57.27
			$2/0/2^{L_m}$	606.86	0.50	220	2.06	$0/2/2^{L_m}$	597.13	0.35	260	0.42
			$8/0/0^{L_l}$	744.71	1.00	80	25.24	$8/0/0^{L_l}$	744.71	1.00	80	25.24
P-n76-k5(280)	635.04	224-280-350	$\mathbf{0/0/4^{L_s}}$	**601.29**	0.00	400	**0.00**	$2/0/5^{L_s}$	974.60	0.29	520	62.09
			$3/0/3^{L_m}$	632.18	0.50	160	5.14	$1/3/2^{L_m}$	646.81	0.52	300	7.57
			$8/0/0^{L_l}$	767.63	1.00	80	27.66	$8/0/0^{L_l}$	767.63	1.00	80	27.66
P-n101-k4(400)	692.28	320-400-500	$\mathbf{0/0/3^{L_s}}$	**679.68**	0.00	300	**0.00**	$3/1/4^{L_s}$	983.43	0.46	460	44.69
			$2/0/2^{L_m}$	711.54	0.50	220	4.69	$2/2/2^{L_m}$	690.92	0.57	280	1.65
			$11/0/0^{L_l}$	1004.26	1.00	110	47.76	$11/0/0^{L_l}$	1004.26	1.00	110	47.76
Average							3.94^{L_s}					45.04^{L_s}
							8.85^{L_m}					4.62^{L_m}
							35.31^{L_l}					27.19^{L_l}

regarding index GI_1. Moreover, MRIG is able to provide routes with a lower cost than the ones in the homogeneous case. This is due to an increase in the loading capacity of vehicles of type *L*. For a randomly selected subset of 20 instances, Figure 5 shows a scatter-plot of distance-based cost (*DBCost*) versus green level (as measured by the GI_1 index). The left point (circle) in each panel represents the best solution in terms of distance-based cost, while the right point (square) represents an alternative 'greener' solution (i.e., one with a higher value of GI_1). Notice that it is usually possible to choose a greener solution without having to assume a noticeable increase in the distance-based cost (instances E-n76-k10, F-n72-k4, P-n101-k4, or P-n40-k5 are good examples). Just in a few cases (e.g., instance M-n121-k7), a noticeable increase in the green level might also require paying a much higher distance-based cost.

Finally, Figure 6 illustrates eight alternative fleet configurations for the A-n45-k7 instance. The auxiliary index $GI_2i = 1/GI_2$ has been employed instead of GI_2 to fa-

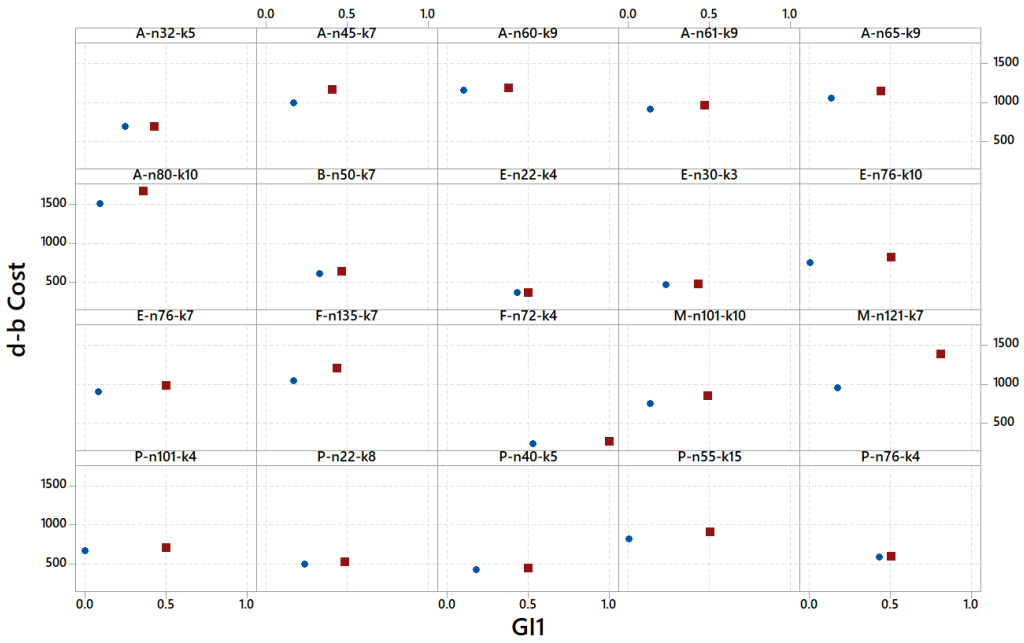

Figure 5: *A comparison of best DBCost solutions (circles) and 'greener' alternatives (squares).*

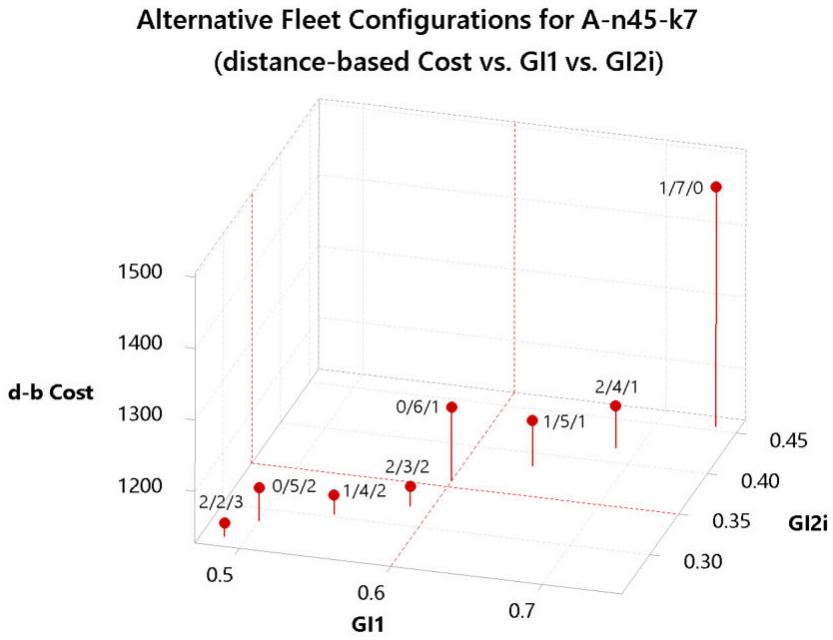

Figure 6: *Cost and green indexes values of eight alternative fleet configurations for instance A-n45-k7.*

cilitate the readability of the figure (i.e., higher values of both GI_1 and $GI_2 i$ represent greener configurations). In this figure, we can see that the best configuration, in terms of distance-based cost, is $2/2/3$. However, the green level of the other solutions is higher. Therefore, the decision-maker could prefer alternative configurations such as $2/3/2$ and $2/4/1$. The latter two solutions offer greener configurations without a significant increase in distance-based cost. This illustrative plot shows how decision-makers can benefit from being able to choose from alternative fleet configurations with different green levels.

8 Conclusion and future work

The paper has introduced a realistic version of the vehicle routing problem in which hybrid fleets of gas and electric vehicles are considered. The introduction of electric vehicles in the model offers clear benefits in terms of making transportation more environment-friendly. However, due to the limited driving-range capabilities of electric batteries, the use of these vehicles also imposes new challenges that need to be solved. We have proposed a novel metaheuristic, MRIG, to solve both the homogeneous and heterogeneous version of the vehicle routing problem with multiple driving ranges. Our MRIG algorithm has outperformed the state-of-the-art results in the case of the homogeneous version. In addition, our approach has been able to solve the heterogeneous version too. This version considers hybrid fleets of vehicles with both different driving ranges and loading capacities.

The metaheuristic is designed to generate a set of fleet configurations with different green levels including small- and medium-driving range electric vehicles instead of gas-fueled vehicles. This solution can be used by decision-makers to help them choose the fleet configuration that fits best with their needs among a set of provided solutions. In some cases, greener configurations might have a higher distance-based cost, but the extensive experiments carried out in this paper showed that it is frequently possible to choose a greener configuration without a significant increase in the distance-based cost. We highlight here some research directions to extend this work, based on considering more realistic variants thus, following a common trend in logistics Solos, Tassopoulos and Beligiannis (2016); Solano-Charris, Prins and Santos (2015). First, we aim to design a multi-objective optimization problem and method Martin et al. (2009) to optimize both the distance-based cost and green level of the fleet configuration. Additionally, we will consider the development of a stochastic model and the corresponding solving approach in the presence of uncertainty (e.g., random demands or random traveling times).

Acknowledgements

This work is jointly supported by the Spanish Ministry of Science (RED2018-102642-T), the Andalusian Government, the National Agency for Research Funding AEI, and ERDF (EU) under grants EXASOCO (PGC2018-101216-B-I00), AIMAR (A-TIC-284-UGR18), SIMARK (PY18-4475) and the Ramón y Cajal program (RYC-2016-19800).

References

AbdAllah, A. M. F., D. L. Essam, and R. A. Sarker (2017). On solving periodic re-optimization dynamic vehicle routing problems. *Applied Soft Computing*, 55, 1–12.

Achtnicht, M., G. Bühler, and C. Hermeling (2012). The impact of fuel availability on demand for alternative-fuel vehicles. *Transportation Research Part D: Transport and Environment*, 17, 262–269.

Almouhanna, A., C. L. Quintero-Araujo, J. Panadero, A. A. Juan, B. Khosravi, and D. Ouelhadj (2020). The location routing problem using electric vehicles with constrained distance. *Computers & Operations Research*, 115, 104864.

Andreatta, G., M. Casula, C. De Francesco, and L. De Giovanni (2016). A branch-and-price based heuristic for the stochastic vehicle routing problem with hard time windows. *Electronic Notes in Discrete Mathematics*, 52, 325–332.

Baldacci, R., M. Battarra, and D. Vigo (2008). Routing a heterogeneous fleet of vehicles. In *The Vehicle Routing Problem: Latest Advances and New Challenges*, Chapter 10, pp. 3–27. Springer.

Belloso, J., A. A. Juan, and J. Faulin (2019). An iterative biased-randomized heuristic for the fleet size and mix vehicle-routing problem with backhauls. *International Transactions in Operational Research*, 26, 289–301.

Brito, J., F. J. Martínez, J. A. Moreno, and J. L. Verdegay (2015). An ACO hybrid metaheuristic for close–open vehicle routing problems with time windows and fuzzy constraints. *Applied Soft Computing*, 32, 154–163.

Calvet, L., A. A. Juan, C. Serrat, and J. Ries (2016). A statistical learning based approach for parameter fine-tuning of metaheuristics. *SORT-Statistics and Operations Research Transactions*, 40, 201–224.

Chan, C. C., Y. S. Wong, A. Bouscayrol, and K. Chen (2009). Powering Sustainable Mobility: Roadmaps of Electric, Hybrid, and Fuel Cell Vehicles. *Proceedings of the IEEE*, 97, 603–607.

Chebbi, O. and J. Chaouachi (2015). Multi-objective Iterated Greedy Variable Neighborhood Search Algorithm For Solving a full-load automated guided vehicle routing problem with battery constraints. *Electronic Notes in Discrete Mathematics*, 47, 165–172.

Clarke, G. and J. W. Wright (1964). Scheduling of Vehicles from a Central Depot to a Number of Delivery Points. *Operations Research*, 12, 568–581.

Crainic, T. G. (2000). Service network design in freight transportation. *European Journal of Operational Research*, 122, 272–288.

Dell'Amico, M., M. Monaci, C. Pagani, and D. Vigo (2007). Heuristic approaches for the fleet size and mix vehicle routing problem with time windows. *Transportation Science*, 41, 516–526.

Dominguez, O., A. A. Juan, I. A. de la Nuez, and D. Ouelhadj (2016). An ils-biased randomization algorithm for the two-dimensional loading hfvrp with sequential loading and items rotation. *Journal of the Operational Research Society*, 67, 37–53.

Erdoğan, S. and E. Miller-Hooks (2012). A Green Vehicle Routing Problem. *Transportation Research Part E: Logistics and Transportation Review*, 48, 100–114.

Faulin, J., S. E. Grasman, A. A. Juan, and P. Hirsch (2019). Sustainable transportation: concepts and current practices. In *Sustainable Transportation and Smart Logistics*, pp. 3–23. Elsevier.

Faulin, J., F. Lera-López, and A. A. Juan (2011). Optimizing routes with safety and environmental criteria in transportation management in spain: a case study. *International Journal of Information Systems and Supply Chain Management*, 4, 38–59.

Feillet, D. (2010). A tutorial on column generation and branch-and-price for vehicle routing problems. *4OR - A Quarterly Journal of Operations Research*, 8, 407–424.

Felipe, N., M. T. Ortuño, G. Righini, and G. Tirado (2014). A heuristic approach for the green vehicle routing problem with multiple technologies and partial recharges. *Transportation Research Part E: Logistics and Transportation Review*, 71, 111–128.

Ferone, D., A. Gruler, P. Festa, and A. A. Juan (2019). Enhancing and extending the classical grasp framework with biased randomisation and simulation. *Journal of the Operational Research Society*, 70, 1362–1375.

Ferreira, J., P. Pereira, P. Filipe, and J. Afonso (2011). Recommender system for drivers of electric vehicles. *ICECT 2011 - 2011 3rd International Conference on Electronics Computer Technology*, 5, 244–248.

François, V., Y. Arda, Y. Crama, and G. Laporte (2016). Large neighborhood search for multi-trip vehicle routing. *European Journal of Operational Research*, 255, 422–441.

Ghannadpour, S. F., S. Noori, R. Tavakkoli-Moghaddam, and K. Ghoseiri (2014). A multi-objective dynamic vehicle routing problem with fuzzy time windows: Model, solution and application. *Applied Soft Computing*, 14, 504–527.

Goeke, D. and M. Schneider (2015). Routing a mixed fleet of electric and conventional vehicles. *European Journal of Operational Research*, 245, 81–99.

González-Martín, S., A. A. Juan, D. Riera, Q. Castellà, R. Muñoz, and A. Pérez (2012). Development and assessment of the sharp and randsharp algorithms for the arc routing problem. *AI Communications*, 25, 173–189.

Hatami, S., R. Ruiz, and C. Andrés-Romano (2015). Heuristics and metaheuristics for the distributed assembly permutation flowshop scheduling problem with sequence dependent setup times. *International Journal of Production Economics*, 169, 76–88.

Hiermann, G., J. Puchinger, S. Ropke, and R. F. Hartl (2016). The Electric Fleet Size and Mix Vehicle Routing Problem with Time Windows and Recharging Stations. *European Journal of Operational Research*, 252, 995–1018.

Hokama, P., F. K. Miyazawa, and E. C. Xavier (2016). A branch-and-cut approach for the vehicle routing problem with loading constraints. *Expert Systems with Applications*, 47, 1–13.

Jie, W., J. Yang, M. Zhang, and Y. Huang (2019). The two-echelon capacitated electric vehicle routing problem with battery swapping stations: Formulation and efficient methodology. *European Journal of Operational Research*, 272, 879–904.

Juan, A. A., J. Faulin, J. C. Cruz, B. B. Barrios, and E. Martinez (2014a). A successive approximations method for the heterogeneous vehicle routing problem: analysing different fleet configurations. *European Journal of Industrial Engineering*, 8, 762.

Juan, A. A., J. Goentzel, and T. Bektaş (2014b). Routing fleets with multiple driving ranges: Is it possible to use greener fleet configurations? *Applied Soft Computing Journal*, 21, 84–94.

Juan, A. A., C. A. Mendez, J. Faulin, J. De Armas, and S. E. Grasman (2016). Electric vehicles in logistics and transportation: A survey on emerging environmental, strategic, and operational challenges. *Energies*, 9, 1–21.

Karakatič, S. and V. Podgorelec (2015). A survey of genetic algorithms for solving multi depot vehicle routing problem. *Applied Soft Computing*, 27, 519–532.

Kek, A. G. H., R. L. Cheu, and Q. Meng (2008). Distance-constrained capacitated vehicle routing problems with flexible assignment of start and end depots. *Mathematical and Computer Modelling*, 47, 140–152.

Keskin, M. and B. Çatay (2016). Partial recharge strategies for the electric vehicle routing problem with time windows. *Transportation Research Part C: Emerging Technologies*, 65, 111–127.

Koç, C. a., T. Bektaş, O. Jabali, and G. Laporte (2016). Thirty years of heterogeneous vehicle routing. *European Journal of Operational Research*, 249, 1–21.

Laporte, G. (2009). Fifty Years of Vehicle Routing. *Transportation Science*, 43, 408–416.

Laporte, G., M. Desrochers, and Y. Nobert (1984). Two exact algorithms for the distance-constrained vehicle routing problem. *Networks*, 14, 161–172.

Li, C.-L., D. Simchi-Levi, and M. Desrochers (1992). On the distance constrained vehicle routing problem. *Operations research*, 40, 790–799.

Lin, J., W. Zhou, and O. Wolfson (2016). Electric Vehicle Routing Problem. *Transportation Research Procedia*, 12, 508–521.

Martin, D., R. del Toro, R. Haber, and J. Dorronsoro (2009). Optimal tuning of a networked linear controller using a multi-objective genetic algorithm and its application to one complex electromechanical process. *International Journal of Innovative Computing, Information and Control*, 5, 3405–3414.

Mattila, T. and R. Antikainen (2011). Backcasting sustainable freight transport systems for Europe in 2050. *Energy Policy*, 39, 1241–1248.

Montoya, A., C. Guéret, J. E. Mendoza, and J. G. Villegas (2014). A multi-space sampling heuristic for the green vehicle routing problem. *Transportation Research Part C: Emerging Technologies*, 70, 113–128.

Osman, I. and C. Potts (1989). Simulated annealing for permutation flow-shop scheduling. *Omega*, 17, 551–557.

Pierre, D. M. and N. Zakaria (2017). Stochastic partially optimized cyclic shift crossover for multi-objective genetic algorithms for the vehicle routing problem with time-windows. *Applied Soft Computing*, 52, 863–876.

Quintero-Araujo, C. L., J. P. Caballero-Villalobos, A. A. Juan, and J. R. Montoya-Torres (2017). A biased-randomized metaheuristic for the capacitated location routing problem. *International Transactions in Operational Research*, 24, 1079–1098.

Reyes-Rubiano, L., D. Ferone, A. A. Juan, and J. Faulin (2019). A simheuristic for routing electric vehicles with limited driving ranges and stochastic travel times. *SORT-Statistics and Operations Research Transactions*, 43, 3–24.

Ruiz, R. and T. Stützle (2007). A simple and effective iterated greedy algorithm for the permutation flow-shop scheduling problem. *European Journal of Operational Research*, 177, 2033–2049.

Ruiz, R. and T. Stützle (2008). An Iterated Greedy heuristic for the sequence dependent setup times flow-shop problem with makespan and weighted tardiness objectives. *European Journal of Operational Research*, 187, 1143–1159.

Schneider, M., A. Stenger, and D. Goeke (2014). The electric vehicle-routing problem with time windows and recharging stations. *Transportation Science*, 48, 500–520.

Solano-Charris, E., C. Prins, and A. C. Santos (2015). Local search based metaheuristics for the robust vehicle routing problem with discrete scenarios. *Applied Soft Computing*, 32, 518–531.

Solos, I. P., I. X. Tassopoulos, and G. N. Beligiannis (2016). Optimizing shift scheduling for tank trucks using an effective stochastic variable neighbourhood approach. *International Journal of Artificial Intelligence*, 14, 1–26.

Vaz Penna, P. H., H. M. Afsar, C. Prins, and C. Prodhon (2016). A Hybrid Iterative Local Search Algorithm for The Electric Fleet Size and Mix Vehicle Routing Problem with Time Windows and Recharging Stations. *IFAC-PapersOnLine*, 49, 955–960.

Verma, A. (2018). Electric vehicle routing problem with time windows, recharging stations and battery swapping stations. *EURO Journal on Transportation and Logistics*, 7, 415–451.

Wang, C., D. Mu, F. Zhao, and J. W. Sutherland (2015). A parallel simulated annealing method for the vehicle routing problem with simultaneous pickup-delivery and time windows. *Computers & Industrial Engineering*, 83, 111–122.

Williams, J. H., A. Debenedictis, R. Ghanadan, A. Mahone, J. Moore, W. R. M. Iii, S. Price, and M. S. Torn (2012). 2050 : The Pivotal Role of Electricity. *Science*, 335, 53–60.

Wirasingha, S. G., N. Schofield, and A. Emadi (2008). Plug-in hybrid electric vehicle developments in the US: Trends, barriers, and economic feasibility. In *2008 IEEE Vehicle Power and Propulsion Conference*, pp. 1–8.

Yu, V. F. and S.-Y. Lin (2015). A simulated annealing heuristic for the open location-routing problem. *Computers & Operations Research*, 62, 184–196.